Geophysical Research Letters

RESEARCH LETTER
10.1029/2019GL084705

Juxtaposition of Western Pacific Subtropical High on Asian Summer Monsoon Shapes Subtropical East Asian Precipitation

Hai Xu[1,2], Yonaton Goldsmith[3,4], Jianghu Lan[2], Liangcheng Tan[2], Xulong Wang[2], Xinying Zhou[5], Jun Cheng[6], Yunchao Lang[1], and Congqiang Liu[1]

[1]Institute of Surface-Earth System Science, Tianjin University, Tianjin, China, [2]State Key Laboratory of Loess and Quaternary Geology, Institute of Earth Environment, Chinese Academy of Sciences, Xi'an, China, [3]Institute of Earth Sciences, The Hebrew University of Jerusalem, Jerusalem, Israel, [4]Division of Geological and Planetary Sciences, California Institute of Technology, Pasadena, CA, USA, [5]Laboratory of Human Evolution and Archeological Science, Institute of Vertebrate Paleontology and Paleoanthropology, Chinese Academy of Sciences, Beijing, China, [6]Nanjing University of Information Science and Technology, Nanjing, China

Abstract Increasing lines of evidence question the homogenous response of Asian Summer Monsoon (ASM) precipitation patterns, requiring rethinking of the forcing mechanisms. Here we show a ~15,000-year quantitative precipitation history based on well-dated lake levels at Lake Chenghai, subtropical China. Lake levels and the inferred precipitation were high during the Bølling-Allerød, early and late Holocene, but low during the middle Holocene. The orbital scale precipitation trend is out of phase with boreal summer insolation, the later has been widely suggested as the driver of ASM precipitation. Lake Chenghai long-term lake levels are synchronous with trends in tropical Pacific sea surface temperatures, the related zonal sea surface temperature gradients, and interhemispheric temperature gradients. We propose that changes in either the interhemispheric or zonal Pacific temperature gradients modulate the intensity and location of the western Pacific subtropical high, which is juxtaposed on the ASM, leading to heterogeneous hydroclimatic conditions over subtropical East Asia.

Plain Language Summary We present a 15,000-year record of southern China precipitation based on well-dated (n=130 radiometric ages) lake level variations of a closed basin lake. The reconstructed long-term southern China precipitation trend is out of phase with boreal summer insolation, which has been shown to drive ASM precipitation, but broadly follows trends in tropical Pacific sea surface temperatures (SSTs), the related zonal SST gradients, and interhemispheric temperature gradients. We propose that changes in either the interhemispheric or zonal Pacific temperature gradients modulate the intensity and location of the western Pacific subtropical high and are juxtaposed on the ASM, leading to heterogeneous hydroclimatic conditions over subtropical East Asia, including an unexpected southern China mid-Holocene drought. The results of this study are unique in that (1) precipitation was robustly reconstructed from beach evidence, which is a first-order measure of the balance between rainfall amount and evaporation. (2) A new mechanism driving long-term precipitation changes over subtropical East Asia is proposed. Providing the mechanism stands, increasing SST gradients under the expected global warming scenario could enhance the role of western Pacific subtropical high and lead to less precipitation over subtropical East Asia.

Key Points:
- A 15,000-year precipitation history over subtropical China was reconstructed based on well-dated (n=130 radiometric ages) lake levels
- Subtropical China precipitation trend does not resemble Asian summer monsoon trend but is synchronized with trends in tropical Pacific SST
- Juxtaposition of western Pacific subtropical high on Asian summer monsoon could have shaped the subtropical East Asian precipitation

Supporting Information:
- Supporting Information S1

Correspondence to:
H. Xu and Y. Goldsmith,
xuhai@tju.edu.cn;
yonig@mail.huji.ac.il

Citation:
Xu, H., Goldsmith, Y., Lan, J., Tan, L., Wang, X., Zhou, X., et al. (2020). Juxtaposition of western Pacific subtropical high on Asian Summer Monsoon shapes subtropical East Asian precipitation. *Geophysical Research Letters*, *47*, e2019GL084705. https://doi.org/10.1029/2019GL084705

Received 26 JUL 2019
Accepted 27 JAN 2020
Accepted article online 29 JAN 2020

1. Introduction

Subtropical Asia is one of the world's most populated regions, thus understanding the response of precipitation to changes in climate forcing is crucial for predicting future water availability. On orbital time-scales, changes in ASM precipitation have been generally assumed to be controlled by changes in boreal summer solar insolation (Cheng et al., 2016; Kutzbach, 1981; Y. J. Wang et al., 2001). However, in recent years increasing lines of evidence question the notion of a uniformly direct response of ASM precipitation to changes in boreal summer solar insolation. For example, Xie et al. (2013) and X. Huang et al. (2018) showed a dry mid-Holocene over central China. These heterogeneous responses emerging from recent data highlight the necessity of a thorough reconstruction of the spatial and temporal precipitation patterns in order to understand their possible driving mechanisms.

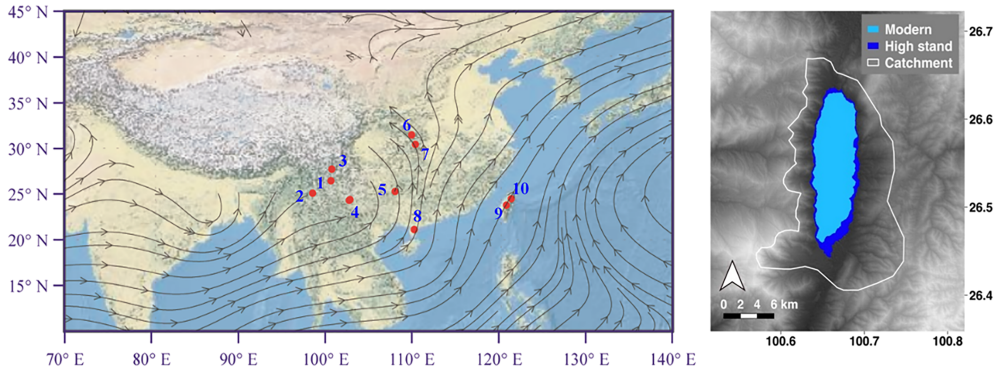

Figure 1. (left) Location of Lake Chenghai and the sites mentioned in the text (see below). The gray arrows show streamlines (at 850 hPa) averaged between June to August of 1968–1996 based on National Centers for Environmental Prediction/National Center for Atmospheric Research reanalysis data (Kalnay et al., 1996). (right) A digital elevation model image of Lake Chenghai with modern and high lake stands, and catchment boundary. The numbers in the left panel denote parts of the sites mentioned in the text: (1) Lake Chenghai (this study), (2) Qinghai Lake in Tengchong County (E. L. Zhang et al., 2017), (3) Lake Lugu (E. L. Zhang et al., 2018), (4) Lake Xingyun and Lake Fuxian (Li et al., 2019; Wu et al., 2018), (5) Dongge Cave (Dykoski et al., 2005), (6) Dajiuhu peatland (Xie et al., 2013), (7) Heshang Cave (Zhu et al., 2017), (8) Lake Huguangyan (HGY; Yancheva et al., 2007), (9) Toushe peat bog (Liew et al., 2006), and (10) Retreat Lake (Selvaraj et al., 2007).

Lake water levels of a closed basin lake are a first-order measure of the balance between precipitation, runoff, and lake evaporation and thus can serve as a quantitative tool to study the variability of regional precipitation and water availability (Broecker, 2010; Goldsmith et al., 2017). In this study, we present the first long-term lake level history at Lake Chenghai (LC), a closed basin lake located in subtropical East Asia (Figure 1; 26.5°N, 100.5°E; Alt. 1,500 m above sea level; also see SI #1; Figure S1 in the supporting information) and discuss the potential mechanisms that dominate precipitation on orbital to millennial timescales over the past ~15,000 years.

2. Methods

2.1. Lake Level Reconstruction

LC receives most of its water vapor from the Indian summer monsoon (SI #1; and Figures S2 and S3). It is situated within a steep flanked pull-apart basin, producing a basin geometry that enables large lake level changes to be driven by small water balance and lake surface area changes, making lake level highly sensitive and enabling a reconstruction of small water balance changes (SI #1; Figure S1). Satellite images (Google Earth) and Shuttle Radar Topography Mission digital elevation model (SRTM DEM; 30-m resolution) were used to locate and map terraces and paleo-shorelines (Figure S1). In the field, 20 outcrops/profiles and 10 paleo-shorelines were mapped and stratigraphic relations were evaluated (SI #2; Figure S4). Eighty-seven radiocarbon ages of pinecones, wood debris, and aquatic snail/mussel shells were obtained (SI #2; Table S1 in the supporting information), and 12 optical stimulated luminescence samples were measured on lake sediments (SI #2; Table S4). In addition, eleven radiocarbon ages of modern samples, including modern lake water, submerged aquatic plant, and living snails (SI #2; Table S2), indicate that lake water is at radiocarbon equilibrium with the atmosphere (SI #2; Table S2), obviating the need for a reservoir correction. Furthermore, a tufa U/Th age is similar to the ^{14}C age of snails from the same layer, strongly supporting the lack of old carbon effect in this lake (SI #2; Table S3). A cave located between the low and high stands at the northeast beach of LC (named "LC Cave" thereafter; SI#3) contains a stalagmite that could not have been formed when the cave was submerged; thus, stalagmite growth episodes indicate times when lake levels were lower than the cave (SI #3; Figure S5). Thirteen U/Th ages were obtained from this stalagmite to cross check the lake level changes inferred from other beach evidence recorded in outcrops/paleo-shorelines (SI #3; Table S3).

2.2. Hydrological Modeling and Lake Level Sensitivity

Changes in the lake's water budget and the sensitivity of lake level to climatic changes were quantified using a mass balance model:

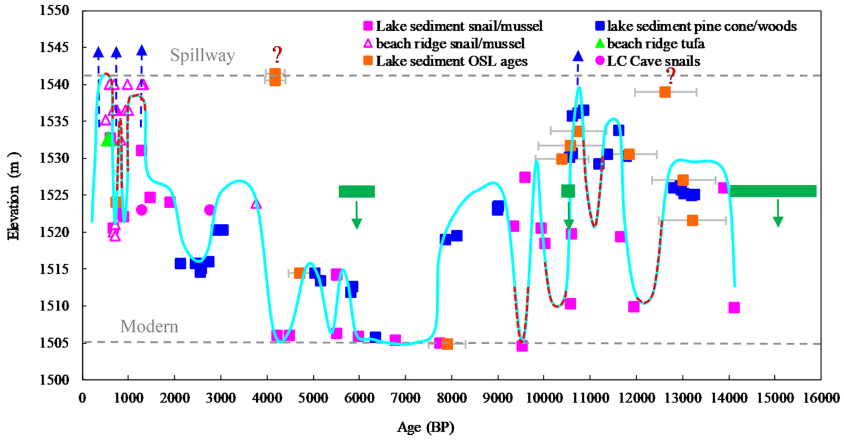

Figure 2. Reconstructed Lake Chenghai lake level curve (blue) and dated material (see legend). The horizontal dashed lines denote the overflow elevation (1,542m) and the modern lake levels (generally at ~1,506m; presently the lake level is <1,500m). The blue arrows show potential lake outflow. The orange question marks denote two potential high stands inferred from optical stimulated luminescence (OSL) ages. The green rectangles with green arrows show the stalagmite U/Th ages, indicating times when the lake was lower than 1,523 m (see SI #3 for details). The red dashed intervals denote times when the extent of low/high stands is uncertain.

$$A_l \times P + (A_c - A_l) \times P \times f = E \times A_l$$

where A_c and A_l are the areas (m^2) of the catchment and the lake, respectively; f is the rainfall utilization fraction (i.e., the percent of rain that reaches the lake as runoff and/or groundwater), and P and E are the precipitation and evaporation (m/year), respectively. For the calculation, we assume the groundwater catchment is identical to the runoff catchment, and therefore, it is included in the calculation of f. Modern f is 22% calculated from modern hydrological observational data (SI #4; Figure S6), which implies that small changes in precipitation could generate big runoff changes.

At the high stand (~40 m above the modern lake level; see below), LC surface area was only ~25% larger than the modern lake area (SI #1). For the high stand, precipitation (P), potential evaporation, and f cannot be constrained independently; therefore, we combined the closed basin lake model with the Fu model (L. Zhang et al., 2004), which is an empirical relation relating E_p, P, and f. To sustain the high stand while assuming potential evaporation was similar to present requires a precipitation increase of ~9% (SI #4). As the lake overflowed at its high stand, this is a minimum value.

Modern evaporation at LC is well modeled by the Penman equation (Linacre, 2009; Figure S2), enabling the use of this equation to test evaporation sensitivity. Global mid-Holocene mean annual temperatures were slightly higher than modern (Marcott et al., 2013); a 1°C higher temperature would increase evaporation by ~20 mm/year, which is 1.3% of the modern evaporation. Thus, we assume that changes in evaporation were negligible and interpret lake level variations as predominantly controlled by changes in precipitation, with higher lake levels corresponding to higher precipitation, and vice versa.

3. Results

3.1. Lake Level Changes at LC

LC lake levels (Figure 2) were 20–40 m higher than present during the Bølling-Allerød (14–12.8 ka) and early Holocene (11.5–8 ka). The high stand is punctuated by four episodes of decreased lake level (12.8–11.5 ka [Younger Dryas], 11±0.2 ka, 10.5–10 ka, and 9.5–9.3 ka). A sharp decrease in lake level occurred at ~8 ka and the lake level remained low for nearly 4,000 years (Figure 2). The LC Cave stalagmite growth episodes occurred at ~16–14 ka BP, ~10.5 ka BP, and during 6.5–5.7 ka BP (Figure 2), consistent with low lake levels inferred from paleo-shoreline/terrace evidence. LC lake levels began rising after ~4 ka BP, and between 2.2 and 0.6 ka BP, lake levels were generally high and the lake overflowed episodically (Figure 2 and Table S1).

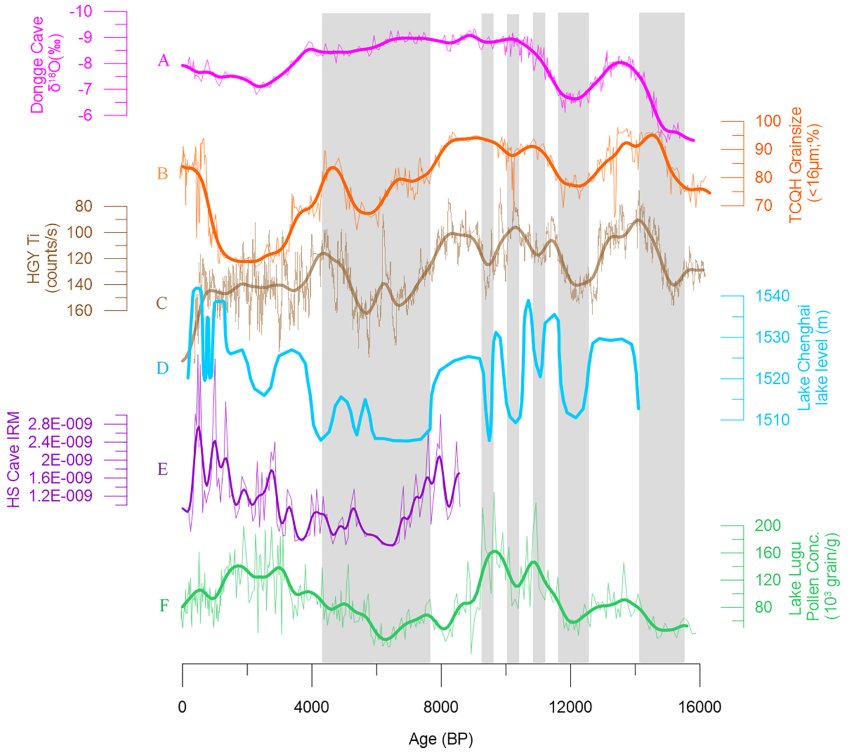

Figure 3. Comparison between Lake Chenghai lake level (curve D; blue thick; this study) and other Asian monsoon proxy indices. (a) Dongge Cave $\delta^{18}O$ curve (pink; Dykoski et al., 2005). (b) Sedimentary grainsize (orange) from Tengchong Qinghai Lake (TCQH; E. L. Zhang et al., 2017). (c) Sedimentary Ti contents (brown) from Lake Huguangyan (Yancheva et al., 2007). (e) Isothermal Remanent Magnetization (IRM) index (purple) from Heshang Cave (Zhu et al., 2017). (f) Pollen concentration (green) from Lake Lugu (E. L. Zhang et al., 2018). The vertical gray columns show broadly synchronous monsoon weakenings between different records from Bølling-Allerød to mid-Holocene.

No beach evidence of high lake levels younger than ~1400 CE was found, which may suggest that the lake could have dropped after that time, or that the strong human activity may remove/mask the natural high lake level beach evidence of the recent several centuries. Historical literature suggests that the lake began to fall during the middle of the Ming Dynasty (1,368–1,644 CE). During the Wanli Empire period (1,573–1,620 CE), a dam (named as "Hai Zha" in Chinese, Alt.: ~1,540 m) was constructed across the Chenghe River as recorded in "Wanli Yunnan Chorography" and "New Yunnan Chorography," suggesting that the lake dropped at that time and people had to artificially store water (Xu et al., 2016; Xu, Song, et al., 2019). A dramatic lake level decrease (~30 m) at ~1,770 CE is described in the chorography of "Yong Bei Zhi Li Ting Zhi" (Hillman et al., 2016; Xu et al., 2016), and the lake switched from an open to closed system thereafter (Xu et al., 2016). However, it is still not clear whether the origin of these lake level drops during the last several centuries is natural or anthropogenic.

3.2. Hydroclimatic Changes at LC

3.2.1. Bølling-Allerød to Early Holocene Wet

The high lake levels from Bølling-Allerød to early Holocene indicate broadly wet hydroclimatic conditions, synchronous with high boreal summer insolation, and coeval with the global deglaciation (14–8 ka). The four sharp decreases in lake levels (12.8–11.5 ka [Younger Dryas], 11±0.2 ka, 10.5–10 ka, and 9.5–9.3 ka) indicate four abrupt monsoon weakenings during this period. These abrupt monsoon weakenings are possibly correlated to events identified in other proxy indices over subtropical East Asia (see comparison in Figure 3).

3.2.2. Mid-Holocene Drought

The mid-Holocene low lake levels indicate dry conditions, which differs from the presently widely recognized wet mid-Holocene conditions inferred from a large number of proxy indices (Dykoski et al., 2005;

Goldsmith et al., 2017; Hudson et al., 2017). However, there are records that support dry mid-Holocene conditions throughout subtropical East Asia (Figures 1 and 3), presented henceforth:

1. Grainsize from Tengchong Qinghai Lake (TCQH; see location in Figure 1), interpreted as an indicator of monsoon precipitation (E. L. Zhang et al., 2017), shows similar trends with LC lake level changes from Bølling-Allerød to the mid-Holocene (Figure 3). A sharp decrease in sedimentary Ti content in TCQH also occurred at ~8 ka and remained low for about 4,000 years (E. L. Zhang et al., 2017), which suggests a dry mid-Holocene hydroclimatic condition (in comparison with the early Holocene). However, during the late Holocene TCQH grainsize record and Ti contents further decreased, which may be ascribed to the strong influences of human activity on the sedimentary records for this small lake.
2. Magnetic index of a stalagmite collected in Heshang cave in Jianghan Basin, central China, showed dry mid-Holocene (Figure 3; Zhu et al., 2017).
3. Transitions from lacustrine sediments to peat deposits during the mid-Holocene in Dajiuhu peatlands (Ma et al., 2009) point to low water availability during the mid-Holocene. Biomarkers indices from these peatlands also suggest much drier conditions during the mid-Holocene (X. Huang et al., 2018; Xie et al., 2013).
4. The sedimentary Ti contents in Lake Huguangyan (HGY) was previously interpreted as dominated by winter monsoon intensity (Yancheva et al., 2007). However, H. Zhou et al. (2007) and Zaarur et al. (2018) argued that the HGY sedimentary Ti should mainly come from the catchment and therefore should be closely related to changes in regional hydrology. Shen et al. (2013) proposed that the HGY sedimentary Ti contents should be controlled by changes in monsoon-dominated vegetation cover and therefore should be inversely correlated to changes in summer monsoon intensities. As shown in Figure 3, the reversed HGY sedimentary Ti contents show a similar trend with the LC lake levels through Bølling-Allerød to mid-Holocene, supporting the monsoon precipitations inferred from LC lake levels. However, the late Holocene HGY Ti contents deviate from the LC lake level trend, this is not surprising as the sedimentation rate nearly tripled during the late Holocene (Yancheva et al., 2007), which may be ascribed to strong anthropogenic impacts on the HGY sedimentary Ti contents.
5. The low total pollen concentrations during the mid-Holocene in Lake Lugu (E. L. Zhang et al., 2018), ~120 km northward to LC, suggest a decrease in vegetation cover and decreased monsoon precipitation over that period (Figure 3). Relatively dry conditions can also be inferred from $\delta^{13}C$ of pyrogenic carbon of the same core (E. L. Zhang et al., 2018).
6. Mid-Holocene dry conditions can also be inferred from the high sedimentary carbonate content (carb%) in Lake Fuxian (approximately 300 km away from LC) and in Lake Xingyun (in adjacent to Lake Fuxian). Sedimentary carb% in both lakes were relatively low (<10%) during the early Holocene but reached 40–60% during the mid-Holocene, and returned to low (~10%) again during the late Holocene (Chen et al., 2014; Hodell et al., 1999; Li et al., 2019; Wu et al., 2018). Lakes Fuxian and Xingyun are closed basin lakes, and thus, increased Carb% could be the result of lake level lowering, causing higher alkalinity and [Ca] and favoring carbonate precipitation. Therefore, the mid-Holocene high sedimentary carb% most likely points to lower water availability and lower lake levels.
7. The monolete spore contents in a core collected at the Toushe peat bog, central Taiwan (Liew et al., 2006; Figure 1), show broadly drier conditions during 8–4 ka BP, in comparison with the early and late Holocene. The switch from lacustrine sediments to peat deposits from early to mid-Holocene in a core collected at Retreat Lake, northeastern Taiwan, also suggests a decreasing water availability during the mid-Holocene, even though it was originally interpreted oppositely (Selvaraj et al., 2007).

3.2.3. Late Holocene Wetting

The high LC lake levels during the late Holocene suggest an increasing trend in precipitation. The fast lake level oscillations inferred from a large number of ages during the interval of 2.2–0.6 ka BP suggest fast and sharp changes in monsoon precipitation. Both the late Holocene wetting trend and precipitation events at LC are similar to those inferred from magnetic index of a stalagmite in Heshang Cave, central China (Zhu et al., 2017).

4. Discussion

LC long-term lake level trend is out of phase with trends in boreal summer solar insolation (Kutzbach, 1981) and precipitation inferred from other proxies (Y. J. Wang et al., 2001) or lake levels (Goldsmith et al., 2017)

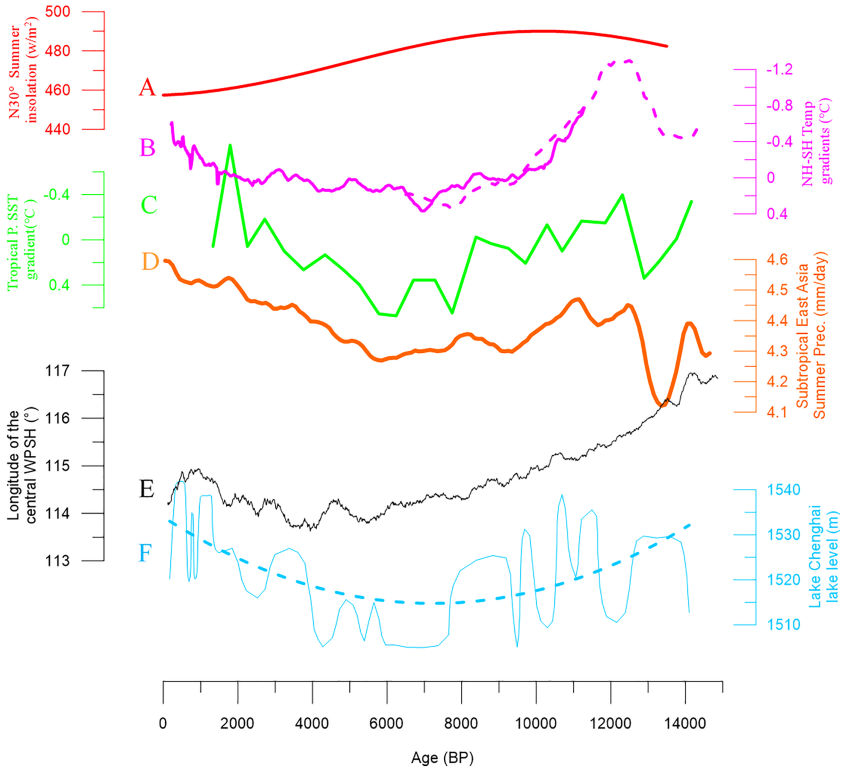

Figure 4. Potential drivers of the long-term subtropical East Asia precipitation. (a) Summer insolation at 30°N (red; Berger, 1978). (b) North-south hemisphere temperature gradients (the pink line is from McGee et al., 2014, and the pink dotted line is from Shakun et al., 2012). (c) Normalized tropical pacific sea surface temperature gradient (green; Koutavas & Joanides, 2012). (d) Simulated summer (June-July-August) precipitation (20–27°N,110–125°E) extracted from TraCE-21ka simulation (orange; Liu et al., 2014). (e) Longitude of the central western Pacific subtropical high (WPSH; black) based on TraCE-21ka simulation (Liu et al., 2014). (f) LC lake levels (blue, this study; the blue-dotted line is the two-order polynomial fit).

from East Asian summer monsoon (EASM) areas (Figure 3), suggesting that additional processes other than direct insolation forcing must have influenced subtropical Asian monsoon precipitation. Millennial scale variability of the ASM has been documented by numerous previous studies and has been ascribed to changes in solar activity and global oceanic circulations (Hong et al., 2003; Y. Wang et al., 2005; Xu et al., 2015); thus, we will not address millennial monsoon variability but focus on the long-term LC precipitation trend and its potential driving mechanisms.

The LC record shows high lake level during the early and late Holocene and low lake levels during the mid-Holocene. This pattern is also evident for subtropical East Asian precipitation in the TraCE-21ka simulations (Liu et al., 2014; Figure 4). There are two global records that show similar patterns to LC record: northern to southern hemispheric temperature gradients ($\Delta T_{N\text{-}S}$; McGee et al., 2014) and eastern to western Pacific sea surface temperature (SST) gradients ($\Delta T_{W\text{-}E}$; Koutavas & Joanides, 2012; Figure 4). During the early and late Holocene, $\Delta T_{N\text{-}S}$ and $\Delta T_{W\text{-}E}$ were small, and during the mid-Holocene, $\Delta T_{N\text{-}S}$ and $\Delta T_{W\text{-}E}$ were large. The processes, interactions, and teleconnections between the global meridional energy transport and the zonal Pacific temperature gradients are at the forefront of the climate and paleoclimate communities and thus will not be solved in this paper. In turn, we will use modern observations to evaluate possible mechanisms that can explain the empirical relations between LC and $\Delta T_{N\text{-}S}$ and $\Delta T_{W\text{-}E}$.

4.1. Possible Influence of Zonal Pacific Temperature Gradients on South China Rainfall-El Niño-Southern Oscillation

Modern changes in tropical Pacific SSTs have been suggested to affect modern rainfall over China (Chang et al., 2000; Chiang et al., 2015; Ding et al., 2008; B. Wang et al., 2013) and thus could have potentially

affected rainfall on longer time-scales. Modern observations reveal that the increased equatorial SST gradient during a La Niña state could strengthen the Walker circulation and lead to increased monsoon precipitation over Indian summer monsoon (ISM) areas; while during an El Niño state, the decreased equatorial Pacific SST gradients lead to decreased Walker circulation and weakened ISM precipitation (Kumar et al., 1999). To explore this relation throughout the Holocene, we used a compilation of tropical Pacific SSTs (Koutavas & Joanides, 2012; Figure 4), which represent El Niño-Southern Oscillation (ENSO) fluctuations —the largest source of interannual scale climate variability in the world. $\Delta T_{W\text{-}E}$ was small during the early and late Holocene and large during the mid-Holocene (Koutavas & Joanides, 2012). Tropical ENSO variability was high during the early and late Holocene and low during the mid-Holocene (Cobb et al., 2013; Koutavas & Joanides, 2012; Mcgregor & Gagan, 2004). LC lake levels vary in a pattern that is similar to that of the $\Delta T_{W\text{-}E}$ (Figure 4) and ENSO variability throughout the Holocene. During the mid-Holocene, $\Delta T_{W\text{-}E}$ were increased (Koutavas & Joanides, 2012; Stott et al., 2004), corresponding to an enhanced La Niña state, which based on the modern analogous (Kumar et al., 1999) should correspond to intensified ISM precipitations. However, we show decreased hydroclimatic conditions over subtropical East Asia during the mid-Holocene, suggesting that the tropical Pacific ENSO influence may be more important on annual to decadal/multidecadal scales (Xu et al., 2016). The observed subtropical East Asian long-term water availability could be mainly ascribed to some other forcing, possibly the location of the WPSH as modulated by zonal tropical Pacific SST gradients and interhemispheric temperature gradients which will be discussed below.

4.2. Possible Influence of Zonal Pacific Temperature Gradients on South China rainfall-WPSH

WPSH is a high-pressure system that resides over the western subtropical North Pacific. Precpitation departures over areas governed by the WPSH are negatively correlated with those over typical EASM areas (e.g., northern China; Ding et al., 2008; B. Wang et al., 2013), which has been generally ascribed to the anticyclonic nature of the WPSH (Chiang et al., 2015; Ding et al., 2008; B. Wang et al., 2013). R. Huang and Sun (1992) showed that for modern climate, warmer (colder) SSTs in the tropical western Pacific lead to stronger (weaker) convective activity in the Philippines, which drive a northeastward (southwestward) shift of the WPSH and cause dry (wet) conditions in south China (primarily in the middle to lower reach of the Yangtze River valley and the Huaihe River valley) and wet (dry) conditions in north China (in the Yellow River). T. J. Zhou et al. (2009) used five AGCM models to examine the relationship between WPSH and tropical SST and suggested that negative heating in the central and eastern tropical Pacific and increased convective heating around the equatorial Indian Ocean-western Pacific drive a westward expansion of the WPSH. In the past ~30 years, the tropical oceans were generally warmer, and the WPSH shifted westward (T. J. Zhou et al., 2009), implying that during warmer conditions, the WPSH tends to move westward. Thus, the modern data suggest that the state of tropical Pacific SSTs can drive changes in rainfall in China via changes in the meridional and zonal location of the WPSH.

LC lake level resembles $\Delta T_{W\text{-}E}$ (Figure 4) and the temperature change in the Eastern Pacific (Koutavas & Joanides, 2012, not shown). Although it is presently not clear how the WPSH varies on longer than decadal timescales and what the relation between $\Delta T_{W\text{-}E}$ and the WPSH is. It is likely that the increased mid-Holocene $\Delta T_{W\text{-}E}$ could have triggered stronger equatorial easterly winds and led to warmer SST conditions of the western tropical Pacific, intensifying convective activity around the Philippines and subsequently modulating both the location and intensity of WPSH, and influencing precipitation over subtropical East Asia. We diagnosed the historical locations of the central WPSH based on the TraCE-21ka simulations (Liu et al., 2014), and the extracted central WPSH longitudes (Figure 4) show that the WPSH extended westward gradually from Bølling-Allerød to mid-Holocene, while after ~4ka, the WPSH shifted from west to east, which is broadly consistent with the LC lake level trend. Therefore, if LC lake levels represent the location of the WPSH, this would imply that on longer time scales, the location of the WPSH is modulated by the zonal temperature gradients of the tropical Pacific.

4.3. Influence of Meridional Temperature Gradients on South China Rainfall

Temperature gradients between the northern and southern hemispheres are important in modulating the meridional location of planetary atmospheric circulations (McGee et al., 2014; Toggweiler, 2009). For example, increased $\Delta T_{N\text{-}S}$ is expected to push the north hemisphere westerlies northward and vice versa (McGee et al., 2014; Putnam & Broecker, 2017; Toggweiler, 2009; Xu, Zhou, et al., 2019), and the north hemisphere subtropical high is also expected to move synchronously. Changes in $\Delta T_{N\text{-}S}$ have been linked to changes in

ocean circulation (Chiang & Bitz, 2005; McGee et al., 2014; Toggweiler, 2009). For modern conditions, although the influence of $\Delta T_{N\text{-}S}$ on ASM rainfall is unclear, there is a possibility that an enhanced (reduced) $\Delta T_{N\text{-}S}$ would shift the WPSH northward (southward). As shown above, in the modern, a northeastward displacement of the WPSH results in reduced rainfall in south China and vice versa. Thus, changes in $\Delta T_{N\text{-}S}$ could potentially change the meridional location of the WPSH and consequently modulate the southern China hydroclimatic conditions, especially on long term timescales. The Holocene $\Delta T_{N\text{-}S}$ resembles LC lake levels, during the early and late Holocene when lake levels were high, $\Delta T_{N\text{-}S}$ was small, which would be consistent with a southward displacement of the WPSH. During the mid-Holocene when lake levels were low, $\Delta T_{N\text{-}S}$ was large, which would be consistent with a northward displacement of the WPSH.

5. Conclusions

We reconstructed a 15,000-year lake level history based on elevated shorelines, which enables a quantitative rainfall reconstruction in south China. Lake levels were high during the early and late Holocene and low during the mid-Holocene. The long-term lake level pattern is similar to interhemispheric temperature gradients and zonal Pacific SST gradients. A compilation of paleoclimate records from across China shows that the early Holocene was wet throughout monsoonal China, suggesting a homogenous response throughout China to a strengthened ASM. During the middle and late Holocene, a heterogeneous hydroclimate pattern existed across China. We suggest that a juxtaposition of the WPSH (i.e., changes of its zonal and meridional location) on the ASM, governed by either the interhemispheric or zonal Pacific temperature gradients, caused the observed differential hydroclimate response across China, including the mid-Holocene drought inferred from our southern China lake level records. As global warming continues, the meridional SST gradients are expected to increase (Rind, 1998), which might cause a northward and perhaps westward shift of WPSH (analogous to the conditions during the mid-Holocene), leading to a decrease in precipitation over subtropical East Asia.

Acknowledgments
We thank Kathleen R. Johnson and another two anonymous reviewers for valuable comments and suggestions. This work is funded by the joint NSFC-ISF research program (NSFC grant 41761144070 and ISF grant 2487/17) and by the program (41672169) supported by the National Natural Science Foundation of China. Data are available via the NOAA online server.

References

Berger, A. (1978). Long-term variations of caloric insolation resulting from the earth's orbital elements. *Quaternary Research*, *9*(2), 139–167.

Broecker, W. (2010). Long-term water prospects in the Western United States. *Journal of Climate*, *23*(24), 6669–6683. <Go to ISI>://WOS:000286553500014

Chang, C. P., Zhang, Y. S., & Li, T. (2000). Interannual and interdecadal variations of the East Asian summer monsoon and tropical Pacific SSTs. Part I: Roles of the subtropical ridge. *Journal of Climate*, *13*(24), 4310–4325. <Go to ISI>://WOS:000165989100006

Chen, F. H., Chen, X. M., Chen, J. H., Zhou, A. F., Wu, D., Tang, L. Y., et al. (2014). Holocene vegetation history, precipitation changes and Indian Summer Monsoon evolution documented from sediments of Xingyun Lake, south-west China. *Journal of Quaternary Science*, *29*(7), 661–674. <Go to ISI>://WOS:000344003500006

Cheng, H., Edwards, R. L., Sinha, A., Spotl, C., Yi, L., Chen, S. T., et al. (2016). The Asian monsoon over the past 640,000 years and ice age terminations. *Nature*, *534*(7609), 640–646. Article. <Go to ISI>://WOS:000378676000027

Chiang, J. C. H., & Bitz, C. M. (2005). Influence of high latitude ice cover on the marine Intertropical Convergence Zone. *Climate Dynamics*, *25*(5), 477–496. <Go to ISI>://WOS:000232909000003

Chiang, J. C. H., Fung, I. Y., Wu, C. H., Cai, Y. H., Edman, J. P., Liu, Y. W., et al. (2015). Role of seasonal transitions and westerly jets in East Asian paleoclimate. *Quaternary Science Reviews*, *108*, 111–129. <Go to ISI>://WOS:000348960000008

Cobb, K. M., Westphal, N., Sayani, H. R., Watson, J. T., Di Lorenzo, E., Cheng, H., et al. (2013). Highly variable El Nino-Southern Oscillation throughout the Holocene. *Science*, *339*(6115), 67–70. https://www.ncbi.nlm.nih.gov/pubmed/23288537, https://doi.org/10.1126/science.1228246

Ding, Y., Wang, Z., & Sun, Y. (2008). Inter-decadal variation of the summer precipitation in East China and its association with decreasing Asian summer monsoon. Part I: Observed evidences. *International Journal of Climatology*, *28*(9), 1139–1161.

Dykoski, C. A., Edwards, R. L., Cheng, H., Yuan, D. X., Cai, Y. J., Zhang, M. L., et al. (2005). A high-resolution, absolute-dated Holocene and deglacial Asian monsoon record from Dongge Cave, China. *Earth and Planetary Science Letters*, *233*(1-2), 71–86. <Go to ISI>://WOS:000228828600007

Goldsmith, Y., Broecker, W. S., Xu, H., Polissar, P. J., deMenocal, P. B., Porat, N., et al. (2017). Northward extent of East Asian monsoon covaries with intensity on orbital and millennial timescales. *Proceedings of the National Academy of Sciences of the United States of America*, *114*(8), 1817–1821. https://www.ncbi.nlm.nih.gov/pubmed/28167754, https://doi.org/10.1073/pnas.1616708114

Hillman, A. L., Abbott, M. B., Yu, J. Q., Steinman, B. A., & Bain, D. J. (2016). The isotopic response of Lake Chenghai, SW China, to hydrologic modification from human activity. *Holocene*, *26*(6), 906–916. <Go to ISI>://WOS:000376305700006

Hodell, D. A., Brenner, M., Kanfoush, S. L., Curtis, J. H., Stoner, J. S., Song, X. L., et al. (1999). Paleoclimate of Southwestern China for the past 50,000 yr inferred from lake sediment records. *Quaternary Research*, *52*(3), 369–380. <Go to ISI>://WOS:000083670800011

Hong, Y., Hong, B., Lin, Q., Zhu, Y., Shibata, Y., Hirota, M., et al. (2003). Correlation between Indian Ocean summer monsoon and North Atlantic climate during the Holocene. *Earth and Planetary Science Letters*, *211*(3-4), 371–380.

Huang, R., & Sun, F. Y. (1992). Impacts of the tropical Western Pacific on the East Asian summer. *Journal of the Meteorological Society of Japan*, *70*(1), 243–256.

Huang, X., Pancost, R. D., Xue, J., Gu, Y., Evershed, R. P., & Xie, S. (2018). Response of carbon cycle to drier conditions in the mid-Holocene in central China. *Nature Communications*, *9*(1), 1369. https://www.ncbi.nlm.nih.gov/pubmed/29636471

Hudson, A. M., Quade, J., Huth, T. E., Lei, G., Cheng, H., Edwards, L. R., et al. (2017). Lake level reconstruction for 12.8–2.3 ka of the Ngangla Ring Tso Closed-Basin Lake System, Southwest Tibetan Plateau. *Quaternary Research*, *83*(1), 66–79. https://www.cambridge.org/core/article/lake-level-reconstruction-for-12823-ka-of-the-ngangla-ring-tso-closedbasin-lake-system-southwest-tibetan-plateau/F5F444C50A1206107CB6665D88A364F6

Kalnay, E., Kanamitsu, M., Kistler, R., Collins, W., Deaven, D., Gandin, L., et al. (1996). The NCEP/NCAR 40-Year Reanalysis Project. *Bulletin of the American Meteorological Society*, *77*(3), 437–471. https://doi.org/10.1175/1520-0477(1996)077<0437:TNYRP>2.0.CO;2

Koutavas, A., & Joanides, S. (2012). El Nino-Southern Oscillation extrema in the Holocene and Last Glacial Maximum. *Paleoceanography*, *27*(4). <Go to ISI>://WOS:000312401900002

Kumar, K. K., Rajagopalan, B., & Cane, M. A. (1999). On the weakening relationship between the Indian monsoon and ENSO. *Science*, *284*(5423), 2156–2159. <Go to ISI>://WOS:000081099300045

Kutzbach, J. E. (1981). Monsoon climate of the Early Holocene: Climate experiment with the Earth's orbital parameters for 9000 years ago. *Science*, *214*(4516), 59–61. https://www.ncbi.nlm.nih.gov/pubmed/17802573

Li, T., Zhang, H., Cai, M., Chang, F., Hu, J., Duan, L., et al. (2019). The composition of carbonate matters in the sediments from Lake Fuxian and significance of paleoclimate and water level changes. *Quaternary Sciences*, *39*(3), 642–654. In Chinese with English abstract

Liew, P. M., Lee, C. Y., & Kuo, C. M. (2006). Holocene thermal optimal and climate variability of East Asian monsoon inferred from forest reconstruction of a subalpine pollen sequence, Taiwan. *Earth and Planetary Science Letters*, *250*(3-4), 596–605. <Go to ISI>://WOS:000242195100014

Linacre, E. T. (2009). Estimating U.S. Class A Pan evaporation from few climate data. *Water International*, *19*(1), 5–14. https://doi.org/10.1080/02508069408686189

Liu, Z., Lu, Z., Wen, X., Otto-Bliesner, B. L., Timmermann, A., & Cobb, K. M. (2014). Evolution and forcing mechanisms of El Nino over the past 21,000 years. *Nature*, *515*(7528), 550–553. https://www.ncbi.nlm.nih.gov/pubmed/25428502, https://doi.org/10.1038/nature13963

Ma, C. M., Zhu, C., Zheng, C. G., Yin, Q., & Zhao, Z. P. (2009). Climate changes in East China since the Late-glacial inferred from high-resolution mountain peat humification records. *Science in China Series D-Earth Sciences*, *52*(1), 118–131. <Go to ISI>://WOS:000264953000012

Marcott, S. A., Shakun, J. D., Clark, P. U., & Mix, A. C. (2013). A reconstruction of regional and global temperature for the past 11,300 years. *Science*, *339*(6124), 1198–1201. https://www.ncbi.nlm.nih.gov/pubmed/23471405, https://doi.org/10.1126/science.1228026

McGee, D., Donohoe, A., Marshall, J., & Ferreira, D. (2014). Changes in ITCZ location and cross-equatorial heat transport at the Last Glacial Maximum, Heinrich Stadial 1, and the mid-Holocene. *Earth and Planetary Science Letters*, *390*, 69–79. <Go to ISI>://WOS:000333998400008

Mcgregor, H. V., & Gagan, M. K. (2004). Western Pacific coral δ18O records of anomalous Holocene variability in the El Niño-Southern Oscillation. *Geophysical Research Letters*, *311*(11), L11204.

Putnam, A. E., & Broecker, W. S. (2017). Human-induced changes in the distribution of rainfall. *Science Advances*, *3*(5), e1600871. https://www.ncbi.nlm.nih.gov/pubmed/28580418, https://doi.org/10.1126/sciadv.1600871

Rind, D. (1998). Latitudinal temperature gradients and climate change. *Journal of Geophysical Research*, *103*(D6), 5943–5971. <Go to ISI>://WOS:000072737800002

Selvaraj, K., Chen, C. T. A., & Lou, J. Y. (2007). Holocene East Asian monsoon variability: Links to solar and tropical Pacific forcing. *Geophysical Research Letters*, *34*(1), 83–91. <Go to ISI>://WOS:000243350800006

Shakun, J. D., Clark, P. U., He, F., Marcott, S. A., Mix, A. C., Liu, Z., et al. (2012). Global warming preceded by increasing carbon dioxide concentrations during the last deglaciation. *Nature*, *484*(7392), 49–54. https://www.ncbi.nlm.nih.gov/pubmed/22481357, https://doi.org/10.1038/nature10915

Shen, J., Wu, X. D., Zhang, Z., Gong, W. M., He, T., Xu, X. M., & Dong, H. L. (2013). Ti content in Huguangyan maar lake sediment as a proxy for monsoon-induced vegetation density in the Holocene. *Geophysical Research Letters*, *40*(21), 5757–5763. <Go to ISI>://WOS:000327810800035

Stott, L., Cannariato, K., Thunell, R., Haug, G. H., Koutavas, A., & Lund, S. (2004). Decline of surface temperature and salinity in the western tropical Pacific Ocean in the Holocene epoch. *Nature*, *431*(7004), 56–59. https://www.ncbi.nlm.nih.gov/pubmed/15343330, https://doi.org/10.1038/nature02903

Toggweiler, J. R. (2009). Shifting Westerlies. *Science*, *323*(5920), 1434–1435. https://www.ncbi.nlm.nih.gov/pubmed/19286540

Wang, B., Xiang, B., & Lee, J. Y. (2013). Subtropical high predictability establishes a promising way for monsoon and tropical storm predictions. *Proceedings of the National Academy of Sciences of the United States of America*, *110*(8), 2718–2722. https://www.ncbi.nlm.nih.gov/pubmed/23341624

Wang, Y., Cheng, H., Edwards, R. L., He, Y., Kong, X., An, Z., et al. (2005). The Holocene Asian monsoon: links to solar changes and North Atlantic climate. *Science*, *308*(5723), 854–857. https://www.ncbi.nlm.nih.gov/pubmed/15879216, https://doi.org/10.1126/science.1106296

Wang, Y. J., Cheng, H., Edwards, R. L., An, Z. S., Wu, J. Y., Shen, C. C., & Dorale, J. A. (2001). A high-resolution absolute-dated late Pleistocene Monsoon record from Hulu Cave, China. *Science*, *294*(5550), 2345–2348. https://www.ncbi.nlm.nih.gov/pubmed/11743199

Wu, D., Chen, X. M., Lv, F. Y., Brenner, M., Curtis, J., Zhou, A. F., et al. (2018). Decoupled early Holocene summer temperature and monsoon precipitation in southwest China. *Quaternary Science Reviews*, *193*, 54–67. <Go to ISI>://WOS:000439674100004

Xie, S. C., Evershed, R. P., Huang, X. Y., Zhu, Z. M., Pancost, R. D., Meyers, P. A., et al. (2013). Concordant monsoon-driven postglacial hydrological changes in peat and stalagmite records and their impacts on prehistoric cultures in central China. *Geology*, *41*(8), 827–830. <Go to ISI>://WOS:000323274600003

Xu, H., Lan, J. H., Sheng, E. G., Liu, B., Yu, K. K., Ye, Y. D., et al. (2016). Hydroclimatic contrasts over Asian monsoon areas and linkages to tropical Pacific SSTs. *Scientific Reports*, *6*, 33177. Article. <Go to ISI>://WOS:000382870700001

Xu, H., Song, Y. P., Goldsmith, Y., & Lang, Y. C. (2019). Meridional ITCZ shifts modulate tropical/subtropical Asian monsoon rainfall. *Science Bulletin*, *64*(23), 1737–1739. https://doi.org/10.1016/j.scib.2019.09.025

Xu, H., Yeager, K. M., Lan, J., Liu, B., Sheng, E., & Zhou, X. (2015). Abrupt Holocene Indian Summer Monsoon failures: A primary response to solar activity? *Holocene*, *25*(4), 677–685.

Xu, H., Zhou, K. E., Lan, J. H., Zhang, G. L., & Zhou, X. Y. (2019). Arid Central Asia saw mid-Holocene drought. *Geology*, *47*(3), 255–258. <Go to ISI>://WOS:000459755700020

Yancheva, G., Nowaczyk, N. R., Mingram, J., Dulski, P., Schettler, G., Negendank, J. F., et al. (2007). Influence of the intertropical convergence zone on the East Asian monsoon. *Nature*, *445*(7123), 74–77. https://www.ncbi.nlm.nih.gov/pubmed/17203059, https://doi.org/10.1038/nature05431

Zaarur, S., Stein, M., Adam, O., Mingram, J., Chu, G., Liu, J., et al. (2018). Late Quaternary climate in southern China deduced from Sr–Nd isotopes of Huguangyan Maar sediments. *Earth and Planetary Science Letters*, *496*, 10–19.

Zhang, E. L., Sun, W. W., Chang, J., Ning, D. L., & Shulmeister, J. (2018). Variations of the Indian summer monsoon over the last 30 000 years inferred from a pyrogenic carbon record from south-west China. *Journal of Quaternary Science*, *33*(1), 131–138. https://doi.org/10.1002/jqs.3008

Zhang, E. L., Zhao, C., Xue, B., Liu, Z. H., Yu, Z. C., Chen, R., & Shen, J. (2017). Millennial-scale hydroclimate variations in southwest China linked to tropical Indian Ocean since the Last Glacial Maximum. *Geology*, *45*(5), 435–438. <Go to ISI>://WOS:000404101300017

Zhang, L., Hickel, K., Dawes, W. R., Chiew, F. H. S., Western, A. W., & Briggs, P. R. (2004). A rational function approach for estimating mean annual evapotranspiration. *Water Resources Research*, *40*(2), 89–97. <Go to ISI>://WOS:000189048900002

Zhou, H., Guan, H., & Chi, B. (2007). Record of winter monsoon strength. *Nature*, *450*(7168), E10–E11. discussion E11. https://www.ncbi.nlm.nih.gov/pubmed/18004318

Zhou, T. J., Yu, R. C., Zhang, J., Drange, H., Cassou, C., Deser, C., et al. (2009). Why the Western Pacific Subtropical High Has Extended Westward since the Late 1970s. *Journal of Climate*, *22*(8), 2199–2215. <Go to ISI>://WOS:000266002800019

Zhu, Z., Feinberg, J. M., Xie, S., Bourne, M. D., Huang, C., Hu, C., & Cheng, H. (2017). Holocene ENSO-related cyclic storms recorded by magnetic minerals in speleothems of central China. *Proceedings of the National Academy of Sciences of the United States of America*, *114*(5), 852–857. https://www.ncbi.nlm.nih.gov/pubmed/28096384, https://doi.org/10.1073/pnas.1610930114